IFAC

Four Reaction Wheels Management: Algorithms Trade-Off and Tuning Drivers for the PROBA-3 Mission

Aymeric Kron[*] Amélie St-Amour[*] Jean de Lafontaine[*]

[*] *NGC Aerospace Ltd, 1650 King Ouest, Bureau 202, Sherbrooke, Québec, J1J 2C3, Canada, (e-mail: ngc@ngcaerospace.com)*

Abstract: Reaction Wheels (RW) are common actuators for three-axis stabilized satellites. This paper deals with the management of a RW assembly where four or more skewed RW are used simultaneously. Four-wheel control is commonly used on spacecraft. This paper contributes to this field by providing an efficient algorithm for attitude control torque distribution with RW angular rate constraint management and by providing the rationales that guide the tuning of this algorithm. Moreover, it defines an algorithm for the angular momentum management of this reaction wheels assembly. Eventually, as proof of concept, it applies these algorithms to a realistic scenario of the PROBA-3 mission using a high fidelity simulator. Results demonstrate that the suggested algorithms are operational and efficient. They can be used and adapted to several types of missions.

Keywords: Spacecraft dynamics, control, guidance and navigation.

1. INTRODUCTION

Reaction Wheels (RW) are common actuators for three-axis stabilized satellites. In principle, this type of spacecraft requires only three non-planar RW to ensure full attitude controllability. In reality, most of the time, in order to provide for redundancy, the Reaction-Wheel Assembly (RWA) includes at least one additional RW. The usual strategy consists in using three of the four RW to realise the control torque (or required angular momentum). However, there are advantages in using four or more skewed RW. This is particularly true for a high-accuracy high-agility mission like PROBA-3.

The PROBA-3 mission aims at demonstrating in-orbit the formation flying technology. For this purpose, the mission consists of two spacecraft, the Coronagraph Spacecraft (CSC) and the Occulter Spacecraft (OSC) flying in a highly elliptical orbit around the Earth (see Peyrard et al. (2013) for details). Each satellite is equipped with four RW. On the one hand, fast large-angle manoeuvres are required to fulfil the mode switching requirements and the demonstration of formation-flight reconfiguration manoeuvres. This implies high agility. On the other hand, stringent pointing requirements (see Table (1)) imply high accuracy.

With the high-accuracy high-agility requirements, it is particularly relevant to use simultaneously the four RW of each spacecraft. Indeed, the enhancement of the angular momentum capability increases the spacecraft agility by allowing fast large-angle manoeuvre. It also contributes to enhancing the pointing accuracy as it reduces the

frequency of attitude-disturbing RW offloading. Moreover, the degree of freedom provided by the fourth wheel allows optimisation of the RW operation point by trading off between margin before saturation and margin before zero angular rate crossing (where stiction occurs, impacting pointing performance).

In this context, this paper addresses the conceptual design of the RWA management algorithms for the PROBA-3 mission and provides a proof of concept by numerical simulation performed on a high fidelity Functional Engineering Simulator (FES).

First, the n (> 3) reaction wheels management problem is stated and solutions from the literature are characterised in a clear mathematical formulation that allows comparison, trade off and selection. In addition, this paper provides rationale, guidelines and techniques for the tuning of the parameters of the selected algorithm. This is the first contribution of this paper.

Then, this paper addresses the autonomous Angular Momentum Management (AMM) of a cluster of n (> 3) reaction wheels. This is the second contribution of this paper.

Finally, as a third contribution, this paper applies these algorithms to the PROBA-3 mission, highlighting the resulting gain in performance.

2. REACTION WHEELS MANAGEMENT

This section addresses the problem of control torque realisation by a cluster of $n > 3$ reaction wheels. First, it states the problem, then it presents the most relevant solutions identified by a literature review and identifies the best algorithm to be used in the context of PROBA-3.

Finally, it provides the technique that allows an efficient tuning of the algorithm.

2.1 Statement of the Problem

When four or more skewed RW are used at the same time, the torque commanded to the reaction wheels expressed in a body-fixed frame, denoted here as the B frame, $\mathbf{T^B}$, i.e. the opposite of the control torque to be applied on the spacecraft, is distributed to the n RW: T_{RW_n}. Linear algebra defines the relationship by Eq. (1).

$$\mathbf{T^B} = \mathbf{C_{BRW}T_{RW}} + \mathbf{C_{BRW}Nt} \tag{1}$$

with:

- $\mathbf{C_{BRW}}$ is the $3 * n$ transformation matrix from RW frame to body-fixed frame. The columns of the matrix correspond to the spin-axis unit vectors of each reaction wheel expressed in the body-fixed frame, with the ith column corresponding to wheel number i.
- $\mathbf{T_{RW}}$ is the vector that concatenates the n RW torque T_{RW_i} $i = 1 \ldots n$.
- $\mathbf{N}$ is the $n * m$ null-space matrix of $\mathbf{C_{BRW}}$ satisfying the null-space property: $\mathbf{C_{BRW}N} = \mathbf{0_{3*m}}$ where $m = n - r$ is the degree of redundancy in the RWA computed knowing n the number of RW and r the rank of $\mathbf{C_{BRW}}$ (for 4 RW: $m = 1$).
- $\mathbf{t} = [t_1 \ldots t_m]$ contains the m null-space scaling parameters.

The control torque is distributed to the n RW by isolating $\mathbf{T_{RW}}$ in Eq. (1). Due to the under-determined nature of the problem, $\mathbf{C_{BRW}}$ is not square and the wheel null-space exists. Therefore, the torque expressed in $\mathbf{B}$ is decomposed into two components in the reaction wheels basis: a torque along the null-space and a torque corresponding to the control torque distributed to the RW.

Thus, the control torque can be allocated to the set of wheels in an infinite number of ways. Indeed, $\mathbf{C_{RWB}}$ that "inverses" $\mathbf{C_{BRW}}$ can be computed in an infinite number of ways. Criteria and selection rules must be defined and applied in order to choose the best one. **This can be considered as the first part of the reaction-wheel management problem.**

Moreover, the torque along the null-space, defined as a function of $\mathbf{t}$, can be used as an additional degree of freedom in dealing with reaction-wheel constraints. For instance, this degree of freedom can be used to control the reaction wheel angular rates around a specific reference angular rate in order to avoid zero crossing and saturation without impacting the spacecraft attitude. Indeed, the control torque has no component in the null-space and by definition a torque that remains in the null-space does not contribute to the torque in $\mathbf{B}$. **Defining a relevant approach to set the torque along the null space in order to manage RW operation constraints can be considered as the second part of the reaction-wheel management problem**.

2.2 Review of the Most Relevant Solutions

The basic solution for this actuator allocation problem is the pseudo-inverse method. This approach consists simply

in computing $\mathbf{C_{RWB}} = \mathbf{C_{BRW}^{pinv}}$ and considering $\mathbf{t} = \mathbf{0}$. The merit of this approach is that the actuator allocation logic is simply a gain matrix because the pseudo-inverse of a matrix exists in an analytic form. By nature of the pseudo inverse, this solution minimises the following l_2-norm:

$$\|\mathbf{T_{RW}}\|_2^2 \tag{2}$$

Thus, the torque realised by the reaction wheels is the minimisation of the control torque module when distributed on the available reaction wheels. It must be noted that the pseudo-inverse distributes the three control torque vector components in the body fixed frame to the n reaction wheels torque vector components such that the null-space component of the reaction wheels torque vector is zero (Rigger (2010)).

It must be also noted that all these equations written with torque are also available with angular momentum. Thus, since the pseudo-inverse is the result of unconstrained l_2-norm optimization, it cannot yield an optimal use of the angular momentum capability (Lim and Miotto (2006)).

Therefore, other solutions based on other criteria have been developed. In Markley (2010), a solution for the computation of $\mathbf{C_{RWB}}$ based on l_∞-norm is proposed and compared to the l_2-norm (pseudo-inverse) solution. While the l_2-norm algorithm finds the distribution of an arbitrary angular momentum among the wheels that minimises the sum of squares of the individual wheel momenta; the l_∞-norm algorithm determines the distribution of an arbitrary angular momentum among the wheels that minimises the l_∞-norm of the vector of the individual wheel momenta, i.e. the maximum of the individual wheel momentum magnitudes.

The l_2-norm optimisation approach does not control the amplitude of each RW momentum. Consequently the momentum storage capacity of a RWA managed by this algorithm depends on the value of the maximum momentum that can be assigned to any wheel for a given commanded angular momentum. Thus, this solution is not optimal. Indeed, an optimal use of the angular momentum capacity of a RWA requires that equal demands be made on all RW. In the case of RW with identical capacities, this is accomplished by the l_∞-norm algorithm. Thus, the l_∞-norm algorithm presents a better momentum storage capacity (in fact the optimal one) than the l_2-norm algorithm. This is of great interest as it maximises the time interval between momentum dumping events, i.e., it reduces the number of time the RW have to be off-loaded over a period of time.

The counterpart of this solution is the complexity of the algorithm. Contrary to the l_2-norm optimisation approach which requires simply computing the pseudo-inverse, the l_∞-norm algorithm computation is not trivial (see for instance Lim and Miotto (2006), Markley (2010), Cadzow (1973)).

All of the discussed algorithms compute $\mathbf{C_{RWB}}$ which optimises l_2-norm or l_∞-norm of Eq. (2). However they cannot accommodate any explicit constraint such as angular-rate magnitude limits of actuators (Lim and Miotto (2006)). Taking advantage of the degree of freedom offered

by the existence of the null space is an alternative to manage optimisation and constraints. This is discussed now.

Considering Eq. (3), the goal of kernel management is to find the null-space scaling parameters of $\mathbf{t}$ that fulfil specific objectives or constraints.

$$\mathbf{T_{tot}^{RW}} = \mathbf{T_{nom}^{RW}} + \mathbf{T_{null}^{RW}} \qquad (3)$$

with

- $\mathbf{T_{nom}^{RW}} = \mathbf{C_{BRW}^{pinv}} \mathbf{T^B}$ is the nominal control torque commanded to the RW by the attitude control algorithm.
- $\mathbf{T_{null}^{RW}} = \mathbf{Nt}$ is the torque along the null space that provides additional degrees of freedom to take into account additional objectives and constraints.

Reckdahl (2000) [1] and Rigger (2010) suggest similar algorithms to control RW speed minimising power by controlling RW speed nullspace components $\mathbf{N^T}\omega$ (where ω is the vector of RW speeds measurements) to zero or user defined target value in the null space ω_{null}^{tgt} by means of a PID controller.

$$\mathbf{t} = PID\left(\omega_{null}^{tgt} - \mathbf{N^T}\omega\right) \qquad (4)$$

It must be noted that Schaub and Lappas (2009) proposes another power-optimal control formulation for the RW kernel management that minimises analytically the instantaneous l_2-norm of the RW power vector (not detailed here).

These algorithms provide a strong added value as they allow controlling the RW angular rate around user-defined objectives far from restricted range of operation (such as limit of saturation or zero angular rate to avoid stiction). However, these algorithms still optimise l_2-norm while, as it has been explained above, it is the l_∞-norm, rather than the l_2-norm, optimisation which presents an optimal momentum storage capacity that prolongs the periods between successive momentum dumping manoeuvres to the maximum possible. Indeed, this approach produces sets of RW speeds whose maximum speed is minimum.

Ratan (2007) modifies the algorithm of Eq. (4) in order to optimise indirectly the l_∞-norm:

$$\mathbf{t} = PID\left(\alpha\right) \qquad (5)$$

with

$$\alpha = f\left(\mathbf{N}, \omega\right) \qquad (6)$$

where Eq. 6 (defined in detail in Ratan (2007)) tends to zero when ω reaches the l_∞-norm optimal solution. Unfortunately, this algorithm suffers from two drawbacks. First, the algorithm behind Eq. (6) is composed of several imbricated "if loops", i.e. its stability cannot be assessed analytically. Moreover, as this algorithm is protected by a US patent, there are restrictions to its use by industry.

At this step, the RW management algorithms have been characterised highlighting their pros and cons. It is time to define the solution for PROBA-3.

---

[1] This reference is a US patent since year 2000, however, this solution has been used at large by space industry for more than 20 years.

2.3 Algorithm Definition and Parameters Tuning Method

Algorithm Selection For PROBA-3, the duration of periods between momentum dumping manoeuvres need to be maximised. At the same time, in addition to the saturation limit constraint, zero-angular rate crossing is unacceptable during fine pointing as stiction will prevent fulfilling the requirements defined in Table 1. The performance indices of this table are defined in ESSB-HB-E-003 (2011).

	X-axis (around LOS) arcsec (1σ)	Y-axis arcsec (1σ)	Z-axis arcsec (1σ)
Absolute Attitude Error (AAE)	300	2.8	2.8
Absolute Attitude Stability (AAS)	30 over 10 sec	0.88 over 10 sec	0.88 over 10 sec
Absolute Attitude Measurement Error (AAME)	30	1.25	1.25
Absolute Attitude Measurement Stability (AAMS)	0.75 over 4hr	0.75 over 4 hr	0.75 over 4hr

Table 1. PROBA-3 Attitude Specifications

These requirements would drive the RW management algorithm selection toward a l_∞-norm optimisation solution that allows specifying a RW angular rate target far from the stiction and saturation ranges. However, the next paragraph shows that, within the realistic context of PROBA-3 (and of many other missions), the practical constraints cause the l_∞-norm approach to have no added value relative to the l_2-norm approach. Consequently, while the l_∞-norm approach is theoretically more relevant, in practice, the l_2-norm approach is better because Eq. (4) does not require an "if loop" but simply basic mathematical operations that allow stability assessment by linear analysis and simple implementation and validation.

Parameters Tuning Considering Eq. (4) or Eq. (5), the parameters to be tuned are the PID gains and the angular rate target ω_{null}^{tgt} (a scalar when $n = 4$) of Eq. (4). The following section characterises the drivers of this tuning.

- **Tuning of ω_{null}^{tgt}.** This parameter shall be set to ensure the maximum margin before zero angular rate crossing and saturation limit. As the four wheels are identical, the target angular rate of each RW shall be defined such that each RW has the same amplitude $\frac{\omega_{sat}}{2}$ where ω_{sat} is the considered limit of saturation. This is formalised by Eq. (7):

$$\left\|\omega_{RW_i}^{tgt}\right\| = \frac{\omega_{sat}}{2} \text{ with } i = 1 \text{ to } 4. \qquad (7)$$

This equation defines the amplitude of each RW target angular rate. Their sign can be set by taking advantage of the null space properties by means of Eq. (8).

$$\omega_{RW}^{tgt} = \frac{\omega_{sat}}{2}\mathbf{N} \qquad (8)$$

This tuning ensures $\omega_{RW}^{tgt} \in Null\left(\mathbf{C_{BRW}}\right)$ with $\omega_{RW}^{tgt} = \left[\omega_{RW_1}^{tgt}\,\omega_{RW_2}^{tgt}\,\omega_{RW_3}^{tgt}\,\omega_{RW_4}^{tgt}\right]^T$. It means that, when the wheels are set by Eq. (8), their angular rates do not contribute to the total angular momentum expressed in the body fixed frame: the algebraic sum of the angular momentum of each RW expressed in body-fixed frame is equal to zero. Once ω_{RW}^{tgt} is set, ω_{null}^{tgt} is defined by Eq. (9).

$$\omega_{null}^{tgt} = \mathbf{N^T}\omega_{RW}^{tgt} \qquad (9)$$

- **Tuning of PID gains.** Considering Eq. (3), $\mathbf{T_{nom}^{RW}}$ and $\mathbf{T_{null}^{RW}}$ are in competition for a limited $\mathbf{T_{tot}^{RW}}$ capa-

bility driven by the RW saturation limit. However, it is obvious that attitude control shall have priority. Therefore, it is relevant to limit the fraction p of $\left(\mathbf{T_{tot}^{RW}}\right)_{max}$ allocated to $\mathbf{T_{null}^{RW}}$. Thus, the maximum control torque dedicated to kernel management shall be limited by the following inequality:

$$\left(\mathbf{T_{null}^{RW}}\right)_{max} = \mathbf{N}PID\omega_{null}^{tgt} \leq \frac{1}{p}\left(\mathbf{T_{tot}^{RW}}\right)_{max} \quad (10)$$

Indeed, the maximum error $\left(\omega_{null}^{tgt} - \mathbf{N^T}\omega\right)_{max} = \omega_{null}^{tgt}$ occurs at the activation of the algorithm (once it is activated, the algorithm reduces the error), i.e. when the wheels are not used and consequently damped by friction up to zero angular rate.

Considering that RW_i is the RW for which $\frac{1}{p}\left(\mathbf{T_{tot}^{RWi}}\right)_{max}$ is the smallest, its corresponding inequality drives the tuning of the PID:

$$PID \leq \frac{1}{p}\frac{1}{N_i\omega_{null}^{tgt}}T_{max}^{RW} \quad (11)$$

where T_{max}^{RW} is the maximum torque that one RW can realise and PID is the transfer function of a PID controller.

Eq. (11) provides an upper bound to set the proportional gain of the PID. Once the proportional gain is set, integral and derivative gains can be tuned as a function of the proportional gain considering usual PID tuning criteria.

Moreover, it must be noted that attitude control requires transient evolution of the RW angular rate around their target rate. The kernel management control shall not react to these variations that are required by the attitude control law. Consequently, the kernel management shall be slower than the attitude control.

These two considerations are the drivers of the tuning of the PID controller. When they are used, the transient of each RW angular rate is dominated by the attitude control loop while the slow kernel management loop impacts essentially the steady state. This last remark is important as it highlights that, in practice, the fact that the transient of the kernel management loop is controlled by an l_∞-norm optimisation algorithm or an l_2-norm optimisation algorithm has only a second order effect that can be neglected.

3. ANGULAR MOMENTUM MANAGEMENT

This section defines the algorithm for the Angular Momentum Management (AMM) of a spacecraft equipped with $n > 3$ reaction wheels. First, it defines the problem. Then, it defines the algorithm.

3.1 Statement of the Problem

The dynamic equation of a spacecraft with thrusters (torque $\mathbf{T_{thr}^B}$), reaction-wheels (angular momentum $\mathbf{h_{RW}^B}$) and perturbations (torque $\mathbf{T_p^B}$) is:

$$\dot{\mathbf{h}}_{tot}^B = \mathbf{T_p^B} + \mathbf{T_{thr}^B} \quad (12)$$

Thus, over a period that lies between t_0 and t:

$$\mathbf{h_{tot}^B} = \mathbf{h_{sc}^B} + \mathbf{h_{RW}^B} = \underbrace{\int_{t_0}^t \mathbf{T_p^B}dt}_{\mathbf{h_p^B}} + \underbrace{\int_{t_0}^t \mathbf{T_{thr}^B}dt}_{\mathbf{h_{thr}^B}} + \mathbf{h_{tot}^B}(\mathbf{t_0}) \quad (13)$$

When the satellite attitude is controlled, the spacecraft angular rate ω_{sc}^B has to track a reference. This means that $\mathbf{h_{sc}^B}$ is constrained. In that case, with the thrusters switched off, only the RW can absorb the variations of the total angular momentum generated by the perturbations. With time, $\mathbf{h_{tot}^B}$ and $\mathbf{h_{RW}^B}$ increase, thereby loading the RW and consequently driving them to their saturation limit or zero angular rate. Therefore, a control algorithm that compensates the secular effects of perturbations must be considered to unload the RW using the thrusters.

3.2 AMM Algorithm

The proposed AMM algorithm inherits from previous PROBA missions (Cote et al. (2010)) with two critical adaptations. For PROBA-3, this algorithm unloads, by means of thrusters, a cluster of 4 RW that are operational simultaneously; while for previous PROBA satellites, only three wheels were running at the same time and were unloaded by means of magnetotorquers.

This algorithm ensures that each $\omega_{RW_i}^B$ is within the user-defined range by directly controlling $\mathbf{h_{tot}^B}$. Without any perturbation, the total angular momentum in an inertial frame remains constant ($\mathbf{h_{tot}^I} = \mathbf{h_{tot_{sp}}^I}$) during the manoeuvres. It is the exchange of angular momentum between the reaction wheels and the spacecraft which results in spacecraft rotation. Therefore, $\mathbf{h_{tot_{sp}}^B}$, the nominal value (or set point) of the total angular-momentum available during the manoeuvre, must be set carefully by preloading the reaction wheels in order to ensure that $\mathbf{h_{sc}^B}$ can evolve as required by the mission while $\mathbf{h_{RW}^B}$ fulfils the RW constraints (zero crossing and saturation).

In order to control $\mathbf{h_{tot}^B}$ about $\mathbf{h_{tot_{sp}}^B}$ despite external perturbations, a control torque shall be generated by the thrusters as a function of $\mathbf{h_{ex}^B} = \mathbf{h_{tot}^B} - \mathbf{h_{tot_{sp}}^B}$. This is ensured by a a proportional/integral controller that considers $\mathbf{h_{ex}^B}$ as the error signal. This offloading control loop is enabled/disabled autonomously by the algorithm of Fig. (1) that compares $\left\|\mathbf{h_{ex}^B}\right\|$ to an upper limit R_{lim} defined as a function of the saturation limit and to a lower limit R_{lim} defined as a function of the precision required for the AMM. Roughly, when the total angular momentum reaches the upper limit, the offloading control loop is enabled until the total angular momentum reaches the lower limit.

4. APPLICATION TO PROBA-3

In order to demonstrate the algorithms and the tuning method, it is implemented within the PROBA-3 Guidance, Navigation and Control software and tested in closed-loop by numerical simulations performed on the high fidelity Functional Engineering Simulator (FES) used to support the analyses of the PROBA-3 mission Phase-B (see Peyrard et al. (2013) for details).
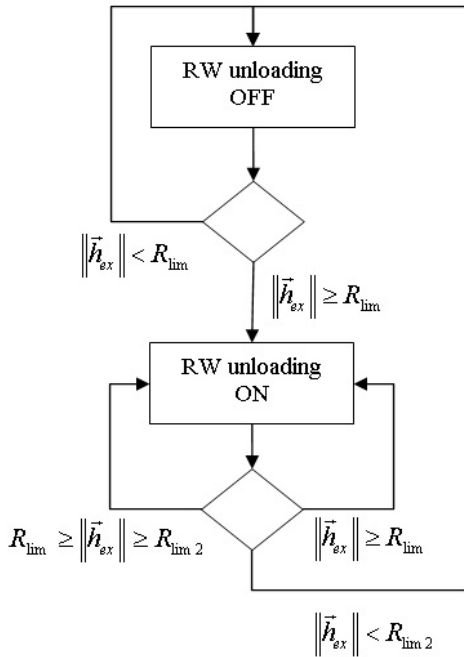
Fig. 1. Angular Momentum Management Algorithm

For the PROBA-3 RWA, $\mathbf{N^T} = [-0.5 \ + 0.5 \ - 0.5 \ + 0.5]$ while the maximum RW angular rate is 526 rad/s. PROBA-3 has no privileged axis of rotation, thus the wheels shall have the same margin before reaching zero or saturation angular rate. It is therefore relevant to set $\omega_{\mathbf{RW}}^{\mathbf{tgt}} = [-263 \ + 263 \ - 263 \ + 263]$, i.e. each wheel has the same margin before reaching zero and saturation limit. This setting drives to $\omega_{null}^{tgt} = 526$ rad/s.

The tuning of the PID is performed using Eq. (11) as an equality for the setting of the proportional gain. For PROBA-3, the maximum torque that one RW can produce is 0.005 Nm while its inertia is 0.0019 kg.m^2. In order to put the emphasis on the attitude control, $p = 10\%$ is selected. This implies that $K_p = 1.9e - 6$. Simulations with this tuning are operational. As required, the kernel management loop is slow. Therefore, in order to put the emphasis on this loop for the present paper, the simulations presented below have been performed with K_p boosted to $K_p = 1.9e - 5$ in order to allow faster convergence (in this context integral and derivative terms have been set to zero).

The scenario of the tests presented in this paper consists in simulations that start with the spacecraft aligned to its target attitude. During the first 1000s, the guidance remains the same. At t=1000s, a 180 deg slew manoeuvre is commanded and, at t =2000s, the original attitude is commanded (i.e. 180 deg manoeuvre to come back). Three tests are performed.

- **Test 1**: 4 RW in the loop without kernel management (i.e. $K_p = 0$) and zero initial RW angular rate.
- **Test 2**: 4 RW in the loop with kernel management (i.e. $K_p = 1.9e - 5$) and zero initial RW angular rate.
- **Test 3**: 4 RW in the loop with kernel management (i.e. $K_p = 1.9e - 5$) and zero RW initial angular rate excepted for RW1 which is set to 450 rad/s, i.e.

inital $\|\mathbf{h_{ex}^B}\|$ is beyond the upper limit R_{lim} thereby requiring offloading.

These tests are analysed through three types of graphs.

- **Graph 1**. The attitude pointing error plots (Fig. (2)) show the overall pointing error between the estimated and target attitude. The three test cases show a similar behaviour where the spacecraft is properly controlled and performs its slew manoeuvres adequately. Thus, the comparison of these three plots highlights that the kernel management does not impact the attitude control. However, the bottom plot shows a loss of precision at the beginning of the simulation during the period of RW offloading. In other words, the thruster activation perturbs the attitude control loop. This behaviour can be avoided by modifying the tuning of the AMM control loop to be slower. Thus, the designer has to trade-off between a slow control that would not impact significantly the attitude pointing and a fast control that shall be performed outside the phases of the mission with tight requirements.
- **Graph 2**. The RW angular rate graphs (Fig. (3)) show the angular rate of each RW. For the case where kernel management is not operational (top plot), the RW drift from their initial values (here zero rad/s) before experiencing a large evolution in order to realise the slew manoeuvres. For the cases where kernel management is activated (middle and bottom plots), it can be observed that before the first slew manoeuvre the RW angular rates evolve rapidly from their initial values to reach their target angular rates tracked by kernel management control. During the slew manoeuvres, the RW angular rates evolve in order to realise the attitude control torque. However, after the manoeuvres the RW are again controlled to their targets without drift. These graphs highlight the need of kernel management in order to load the RW to target angular rates to provide margin relative to zero angular rate and saturation limit. They also highlight that the proposed kernel management and tuning are operational and behave as predicted by the theory.
- **Graph 3**. The AMM graph (Fig. (4)) is used only for **Test 3** where RW offloading is required. It shows the module of the controlled angular momentum and the flag that characterises if the RW offloading is triggered on or off. As the total angular momentum is beyond its upper limit when the simulation starts, the flag is on and the angular momentum is reduced. The algorithm automatically stops when the angular momentum reaches its target value. These plots highlight that the angular momentum management is operational and compatible with the attitude control and kernel management.

5. CONCLUSION

This paper presented algorithms for the management of a cluster of $n > 3$ reaction wheels. It first characterises an efficient algorithm for attitude control torque distribution with RW angular rate constraint management and provides the rationale that guides the tuning of this algorithm. Then, it defines an algorithm for the angular momentum management of this reaction wheel assembly.

Finally, as proof of concept, it applies these algorithms to a realistic scenario of the PROBA-3 mission using a high-fidelity simulator. Results demonstrate that the suggested algorithms are operational and efficient. They can be used and adapted to several types of missions.
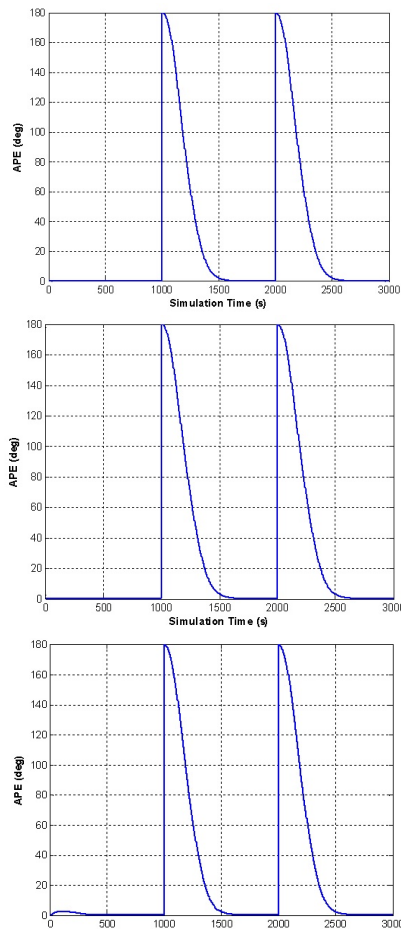

Fig. 2. Attitude Pointing Error - top: $K_p = 0$, Mid.: $K_p = 1.9e - 5$, Bot.: AMM Required

ACKNOWLEDGEMENTS

REFERENCES

Cadzow, J. (1973). A finite algorithm for the minimum l_∞ solution to a system of consistent linear equations. *SIAM J. Numer. Anal., Vol 11, No 6., September 1973*, 11.

Cote, J., Naudet, J., Kron, A., Santandrea, S., and de Lafontaine, J. (2010). Proba-2 attitude and orbit control system: In-flight validation results. In *CASI ASTRO 2010*. Toronto, Canada.

ESSB-HB-E-003 (2011). ESA pointing error engineering handbook. ESSB-HB-E-003, Iss1 Rev0.

Lim, S. and Miotto, P. (2006). Actuator allocation algorithm using interior linear programming. In *AIAA GNC Conference, 21-24 Aug 2006*. Keystone, USA.
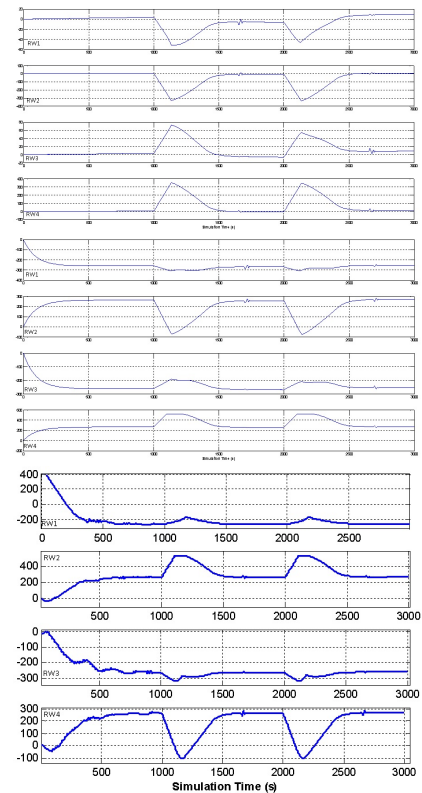

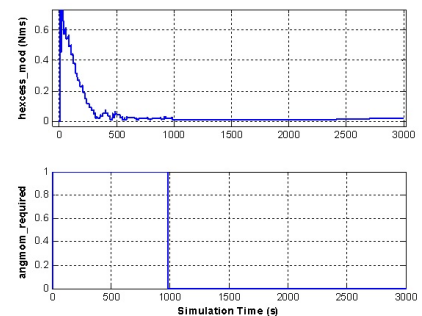Fig. 3. RW Angular Rate $[rad/s]$ - top: $K_p = 0$, Mid.: $K_p = 1.9e - 5$, Bot.: AMM Required

Fig. 4. Controlled Angular Momentum and RW Dumping Required Flag: $K_p = 1.9e - 5$ and AMM Required

Markley, F. (2010). Maximum torque and momentum envelopes for reaction-wheel arrays. *Journal of Guidance Control and Dynamics*, 33.

Peyrard, J., Barrena, V., Branco, J., Agenjo, A., Kron, A., Olmos, D.E., Castellani, L.T., and Cropp, A. (2013). The formation flying software of proba-3. In *7th Internation Workshop on Satellite Constellations and Formation Flying*. Lisbon, Portugal.

Ratan (2007). Optimal speed management for reaction wheel control system and method. US Patent No: 7198232.

Reckdahl (2000). Wheel speed control system for spacecraft with rejection of null space wheel momentum. US Patent No: 6141606.

Rigger, R. (2010). On stiction, limit and constraint avoidance for reaction wheel control. In *SpaceOps 2010 Conference*. Huntsville, Alabama, USA.

Schaub, H. and Lappas, V. (2009). Redundant reaction wheel torque distribution yielding instantaneous l2 power-optimal attitude control. *Journal of Guidance Control and Dynamics*, 32.